Bioculture
Bioculture Journal
Bioculture 3(2): 143–169
ISSN 3025-3632

Institute for Advanced Science, Social and Sustainable Future
MORALITY BEFORE KNOWLEDGE

# Exploring the role of biomass-derived carbon quantum dots: Hydrothermal carbonization, bioimaging in vivo/in vitro, and biomedical application

**Yuni Aldriani Lubis**[1,2,*]
[1] *Postgraduate School, Department of Chemistry, Faculty of Mathematics and Natural Sciences, Universitas Sumatera Utara, Jl. Bioteknologi No.1, Medan, North Sumatera 20155, Indonesia;*
[2] *Cellulosic Functional Material Research Center, Universitas Sumatera Utara, Jalan Bioteknologi No. 1, Kampus USU, Padang Bulan, Medan, North Sumatera 20215, Indonesia.*
*Correspondence: yunialdrianil@gmail.com

Received Date: January 1, 2025 Revised Date: January 25, 2026 Accepted Date: January 27, 2026

## ABSTRACT

**Background:** Carbon-based nanoparticle classes consisting of various subgroups based on morphology and crystallinity are called carbon dots (CQDs). The physical, chemical, and optical properties of CQDs can be modified using the simple pot synthesis technique. Additionally, its non-toxic nature, biocompatibility, physical and chemical responsiveness, resistance to chemical and photo bleaching, and low cost make it suitable for various purposes, such as biomedical imaging applications. Biomass waste, which has been widely discarded without economic utilization and potential, can surprisingly be used as a precursor for CQDs. **Method:** The literature was systematically collected from major databases. Studies from 2017–2025 were analyzed based on synthesis strategies, surface functionalization, and biological performance. Its potential in the medical field is highly advantageous. CQDs have fluorescence that is useful for biomedical imaging both in vivo and in vitro. The hydrothermal carbonization approach is also discussed in more detail, highlighting its green and sustainable synthesis, as well as the ease of the synthesis process. **Finding:** It was found that CQDs have compatibility and adjustable optical properties. Its fluorescence can clearly record tissues, body care, aging, and living cells. Utilizing renewable biomass precursors offers an environmentally friendly and cost-effective route for synthesizing fluorescent nanoprobes with excellent water solubility, tunable emission, and low cytotoxicity. Additionally, in vitro studies reinforce CQDs as multicolor fluorescent probes, and in vivo studies demonstrate that CQDs have low toxicity, rapid clearance, are safe, and biocompatible. **Conclusion:** This paper delves into the remarkable potential of CQDs to provide insights into how fluorescent inks are truly essential in biomedical imaging. **Novelty/Originality of this article:** This study provides a comprehensive and updated synthesis of CQD research spanning up to 2025, specifically focusing on the transition from "waste to nanoprobe."

**KEYWORDS**: carbon quantum dots; bioimaging; In vivo; In vitro; biomass.

## 1. Introduction

With the advancement of technology to date, bioimaging based on sensing and fluorescence imaging has become a trend in medical and biological research (Bian et al., 2025). In vivo and in vitro practices have become widespread in the fields of medicine and biology, and often require specific techniques such as fluorescence imaging, magnetic resonance imaging (MRI), and computed tomography (CT). These techniques enable the

**Cite This Article:**
Lubis, Y. A. (2026). Exploring the role of biomass-derived carbon quantum dots: Hydrothermal carbonization, bioimaging in vivo/in vitro, and biomedical application. *Bioculture Journal, 3*(2), 143-169. https://doi.org/10.61511/bioculture.v3i2.2026.3206

imaging of tissues, organs, glands, and blood vessels, and provide anatomical and molecular information about the objects being analyzed (Leary & Key, 2014; Sturabotti et al., 2025), which requires a confocal fluorescence microscope and bright field, clear, and color images in cellular imaging (Karuppasamy et al., 2025a). However, the development of new fluorescence-based optical materials is still limited. Nanotechnology has emerged and provided innovative solutions in the development of biomedical research, therapy, and disease monitoring (Alhussaini et al., 2026; Haleem et al., 2023; Malik et al., 2023). Among the wide range of nanomaterials, carbon quantum dots (CQDs) are gradually overcoming these challenges in a sustainable manner.

CQDs is a carbon-based family with a size below 10 nm, high biocompatibility, low cost, exceptional functionalization ease, good water solubility, non-toxicity, and good photoluminescence (Chen et al., 2025a; Fang et al., 2024; Wechakorn et al., 2025; Zhou et al., 2019). Due to its many uses, CQDs has been widely used in various applications, including bioimaging, due to its photoluminescence, ease of preparation, and affordability (Das et al., 2024; Feng et al., 2021; Kausar, 2019; Molaei, 2019; Pathak et al., 2023; Wang et al., 2022). Contributors such as metals tend to have toxic effects and are expensive. In addition, metal-based CQDs contributors do not provide high benefits because CQDs function as stabilizing and reducing agents for metals, making CQDs functionalization in bioimaging less than optimal (Hota & Iyer, 2024). Metal nanostructures and other semiconductor materials can also hinder practical applications in the medical field (Chen et al., 2025b), Meanwhile, the synthetic route that produces red fluorescent CQDs also does not offer significant advantages, as it involves organic and toxic solvents, making it less environmentally friendly when used in bioimaging applications (Chen et al., 2025b; Zheng et al., 2020). To overcome this challenge, pure CQDs made from renewable biomass are very promising.

The production of carbon materials from biomass not only utilizes good waste management and handling. However, biomass offers many advantages such as being abundant in nature, economical, non-toxic, environmentally friendly, and reducing the cost of preparing carbon material synthesis (Yuan et al., 2024). This biomass can reduce the potential for unwanted hazardous waste (Duan et al., 2024). The following is data on the percentage of biomass waste production in developed countries as shown in Figure 1.

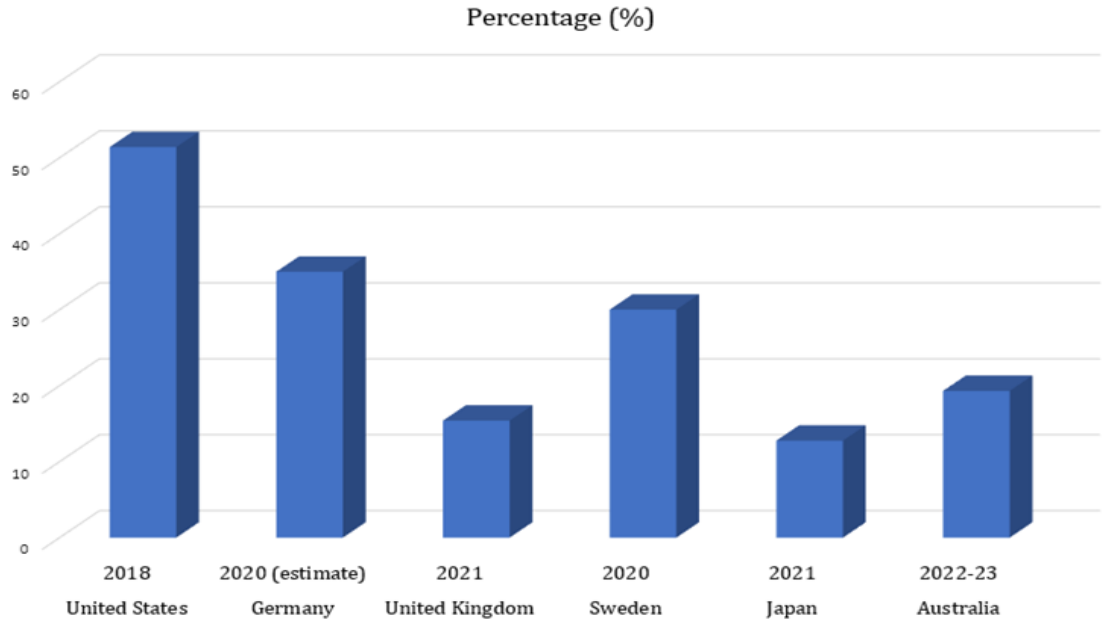


Fig. 1. Percentage of biomass waste in developed countries. Sources: EPA composting/MSW facts, BMUV/EEA country factsheets, DEFRA/Local authority collected waste, Swedish waste management report, MOE Japan food loss & waste and total waste, National waste & resource recovery report 2024, and National Waste Report 2022 (United States Environmental Protection Agency, 2024)

Carbon dots synthesis can be performed using two approaches, namely top-down and bottom-up. The top-down approach involves breaking down large carbon structures into CDs particles using techniques such as laser ablation and chemical oxidation, although this method often produces particles of inconsistent sizes. Conversely, the bottom-up approach includes pyrolysis, hydrothermal, and solvothermal methods (Stachurski et al., 2020). The hydrothermal method is a simple, environmentally friendly process that can produce high-quality CQDs (Mohammed et al., 2024). CQDs synthesis from natural materials such as citric acid generally produces low QY values and suboptimal fluorescence intensity. To improve its optical properties, surface modification and doping with heteroatoms are performed. One widely used approach is doping with non-metallic elements, especially nitrogen. According to research (Lee et al., 2024), The addition of nitrogen through urea precursors not only increases the nitrogen content in the CQDs structure but also acts as a surface passivation agent that covers defects on the particle surface. This process improves fluorescence properties and increases QY from 13.45% to 22.26%. Furthermore, the use of urea as a nitrogen source is considered efficient, low-cost, and has low toxicity, making it suitable for biological and environmental applications.

Biomass for CQDs precursors in medical imaging science has been widely offered. However, further discussion related to medical imaging in health is still limited. Here, we have comprehensively discussed biomass used as CQDs in various applications, in vivo and in vitro imaging, and the potential of CQDs in the world of health. We also limit our discussion to the scope of biomass potential and its performance in bioimaging. This paper has also carefully classified fluorescent probes in in vivo and in vitro bioimaging. This paper provides a significant range of biomass uses designed to enhance its performance in imaging. This paper is expected to provide knowledge and references to researchers and young scientists to develop CQDs from renewable biomass with superior bioimaging capabilities and future potential.

## 2. Methods

### *2.1 Literature search strategy and data analysis*

This study was conducted using a systematic literature review to summarize the latest developments regarding Carbon Quantum Dots (CQDs). Data were collected from various major scientific journal databases covering the publication period from 2017 to 2025. The keywords used in the search included “carbon dots,” “biomass-derived CQDs,” “hydrothermal carbonization,” and “biomedical imaging.”

The selected studies were then screened based on their relevance to the research focus, namely the transition from biomass waste to nanoprobes. The main analysis criteria included synthesis strategies, reviewing various simple pot synthesis techniques, particularly hydrothermal methods. Physicochemical characteristics, analyzing surface functionalization modifications, optical properties (fluorescence), and crystallinity levels. Biological performance, evaluating aspects of cytotoxicity, biocompatibility, and clearance mechanisms within biological systems.

### *2.2 Focus on the evaluation of biomedical applications and sustainable synthesis*

The analytical methods focus on the effectiveness of CQDs as biomedical imaging agents. The evaluation examines the performance of CQDs in in vitro (on living cells) and in vivo (in tissues/organisms) studies, with particular attention to tissue imaging capabilities, aging monitoring, and their potential use as safe and environmentally friendly fluorescent dyes. This research pays special attention to the hydrothermal carbonization method. This technique is analyzed in greater depth due to its advantages in terms of sustainability, ease of process, and efficiency in converting renewable biomass precursors into functional nanoparticles with high water solubility.

## 3. Results and Discussions

### *3.1 Biomass-precursor of CQDs synthesized*

The biomass-derived CQDs precursor is a key foundation for sustainable and functional CQDs in bioimaging applications. Compared to other precursors, biomass not only offers renewability but also structural complexity, compositional diversity, and heteroatoms (Huang et al., 2025). Considering the concept of green synthesis, several objectives can be achieved using biomass precursors: the method is safe to use, it uses safe solvents, it reduces the use of harmful substances, and the synthesis process is safer and less hazardous (Parray et al., 2026). Carbon dots made from biomass are more environmentally friendly and support sustainable development goals 12 and 13. This concept promotes the use of sustainable raw materials and reduces the potential for hazardous waste. Additionally, it supports the use of carbon-neutral biomass and the transition toward sustainable nanomaterials in biomedical imaging applications. The selection of biomass precursors was driven by the large amount of ineffective waste disposal, resulting in waste that lacks high economic value. Waste utilization affects sustainable resources and ecological issues, so to reduce its impact, its use is considered potential waste, such as carbon dot precursors (Krishnaiah et al., 2025).

Biomass has a wide range of uses, including the following. Complex section: chenpi (Xiang et al., 2023), cantaloupe peel (Guo et al., 2025), peanut shell (Yang et al., 2025), orange juice (Solis Flores et al., 2024), oil palm fronds (OPF) (Sambudi et al., 2025), R. Damascene Mill flower residue (Liu et al., 2025c), soybean (Gao et al., 2025), palm kernel shell (Kumar et al., 2024), starch (Liu et al., 2025b), neem (Basha et al., 2024), watermelon rind and grape pomace (Chávez-García et al., 2024), ranting hawthorn (Sun et al., 2025), ginkgo leaves (Mou et al., 2021), Hydrogenated L-glucose (Zhou et al., 2020), dragon fruit peel (Ngara et al., 2025), chrysanthemum, honeysuckle, and artemisinin (Liu et al., 2025a).

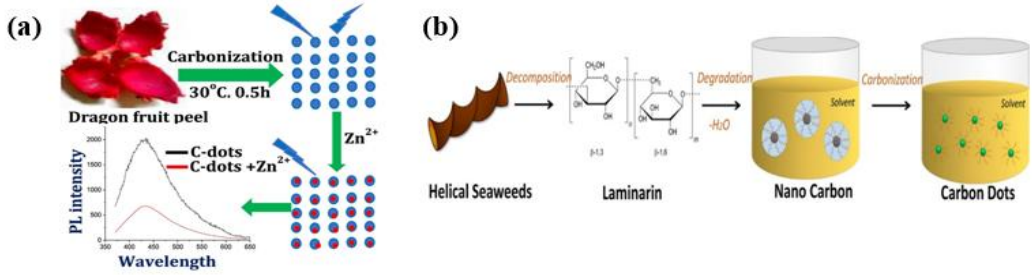


Fig. 2. (a) Carbonization process, copyright 2025, Elsevier (Ngara et al., 2025), and (b) Stages of carbonization, copyright 2023, ACS Sustainable Chemistry & Engineering (Chen et al., 2023)

Simple biomass components: citric acid (Louw et al., 2025), chitosan (Fan et al., 2025), succinic acid (Altaylı et al., 2025), natural protein (Cai et al., 2025), dehydroabietic acid (Huang et al., 2022), cellulose and lignin (Chen et al., 2022), craft lignin (Papan Djaniš et al., 2026), sucrose (Yoda et al., 2026). In the process of synthesizing CQDs using biomass, its use is certainly impractical. This process involves preparation and carbonization stages as shown in Figure 2, thereby avoiding impurities and unwanted components despite its environmentally friendly and low-cost nature. During the carbonization process, several processes occur, including decomposition, degradation, the formation of small fragments, and carbonization to form fluorescent CQDs as shown in Figure 2.

### *3.2 Hydrothermal carbonization and characterization*

Biomass-based carbon dot synthesis often involves several stages. This approach is often referred to as hydrothermal carbonization (HTC). Due to its good water solubility and

hydrophilicity, the hydrothermal carbonization approach is chosen based on these advantages. These characteristics help various molecules and ions to disperse well in the reaction environment. Within the confines of a closed pressure vessel, under high temperature and pressure, biomass undergoes various transformations, such as passivation, polymerization, aromatization, and condensation, which include hydrolysis, dehydration, and decarboxylation processes (Ashraf & Karahan, 2024; Huang et al., 2025). This process of forming CQDs begins with carbonization (Ahn et al., 2024).

Table 1. CQDs from biomass using the HTC method

| Biomass | Temperature and Reaction time | Particle size (nm) | Application |
|---|---|---|---|
| Papaya peel waste (Shahraki et al., 2023) | 200 ℃, 24 h | 4.5 | photocatalytic and antibacterial |
| Banana, curcumin, and orange peels (Patel et al., 2024) | 180 and 200 ℃, 24 h | 2.3 and 3.6 | Antimicrobial and antioxidant |
| Leftover Kiwi Fruit Peel (Atchudan et al., 2021) | 200 ℃, 24 h | 5.6 and 5.1 (based on two calculations) | Sensor |
| Banana peels (Wijayanti et al., 2024) | 135°C, 24 h | 1.8 and 5.4 | Bioimaging |
| Pomegranate peels (Eskalen et al., 2024) | 175 °C, 12 h | 6.5 | Sensor |
| Mangosteen peel (Amloy et al., 2024) | 200°C, 3 h | 3.1 | Biomaging |
| Luochuan Red Fuji Apple Peel (Zhao et al., 2021) | 200°C, 18 h | - | Sensor |
| Marigold flower (Pal et al., 2025) | 140 °C, 6 h | 2–5 | Wound healing |
| German Chamomile Flower and Residual | 200 °C, 6 h | 2.1–7 | Preservative |
| Lantana camara (Mahto et al., 2025) | 250 °C, 5 h | 2.4 | Sensor and bioimaging |
| Neem (Azadirachta indica) leaves (Gedda et al., 2023) | 180 °C, 12 h | 3.5 | Antimicrobial, antioxidant, and bioimaging |
| Peltophorum pterocarpum flowers (Vinayagam et al., 2025) | 220 °C, 4 h | 3.4 | Sensor |
| Herbal medicine (Luo et al., 2021) | 300 °C, 2 h | 1.3 | Bioimaging |
| Momordica charantia L. (Liu et al., 2021) | 180 °C, 5 h | 8.5 | Sensor |

HTC often offers several advantages such as environmentally friendly precursors, mild reaction conditions, non-toxicity and no pollution, lower reaction temperatures, low cost efficiency, simple synthesis processes, and suitability for large-scale synthesis (Naziba et al., 2024; Owsianiak et al., 2016; Sun & Li, 2004; Wang et al., 2001). In addition, CQDs from biomass with HTC has been widely applied based on the following table. After the material is synthesized, it will be characterized to determine its optical properties, electronic structure, morphology, surface functional groups, and particle size distribution. CQDs characterization techniques are divided in Table 1.

### *3.2.1 Fluorescence spectrophotometer*

Photoluminescence is a process in which a material absorbs light and causes its electrons to rise to a higher energy level. When the electrons return to their original energy level, light is emitted as a result. Fluorescence spectrophotometers are used to evaluate the color and wavelength of light emitted by CQDs. This technique is based on the basic principles of light absorption and emission. When CQDs are exposed to light of a certain

wavelength, the electrons within them absorb energy from the photons and move to a higher energy level. Subsequently, the electrons return to their ground state and emit light, known as fluorescence (Jing et al., 2023).

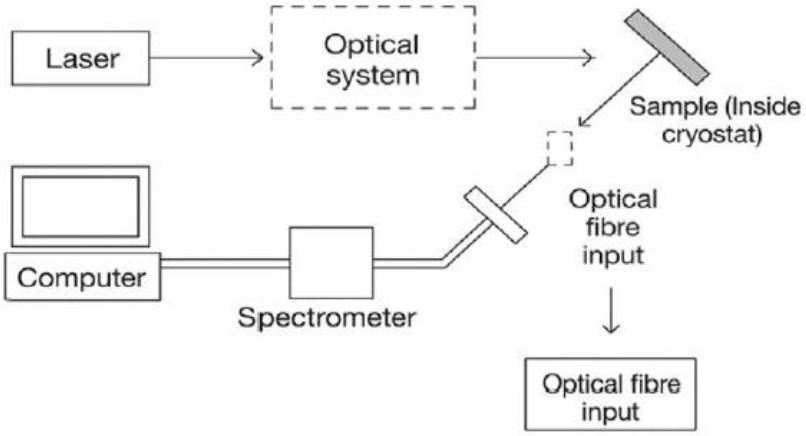


Fig. 3. Photoluminescence technique works, copyright 2019, The Royal Society of Chemistry (Ren et al., 2019)

The PL technique is widely used to identify the characteristic emission of CQDs due to their attractive optical properties, both fundamentally and applicationally. CQDs show advantages over other fluorescent materials, such as high light stability, low toxicity, low synthesis cost, and good biocompatibility. The intensity of PL emission in CQDs depends on the QY, which is influenced by the carbon source, synthesis method, and surface modification. In addition, the absorption and emission characteristics of CQDs are greatly influenced by the type and number of surface functional groups, and the oxygen and nitrogen content in the carbon core (Liu et al., 2020).

### *3.2.2 Spektrofotometer UV-Visible*

UV-Vis spectrophotometers are often used to study the optical properties of CQDs, because CQDs made by various methods usually show strong absorption in the UV region, although the position of the absorption peak may vary. This method works based on the principle of ultraviolet or visible light absorption by a substance, which produces a specific spectrum as shown in Figure 4. When light is absorbed, electrons in the substance undergo excitation and then return to their initial state (de-excitation), which produces a spectral pattern as a result of the interaction between light and matter (Jing et al., 2023).

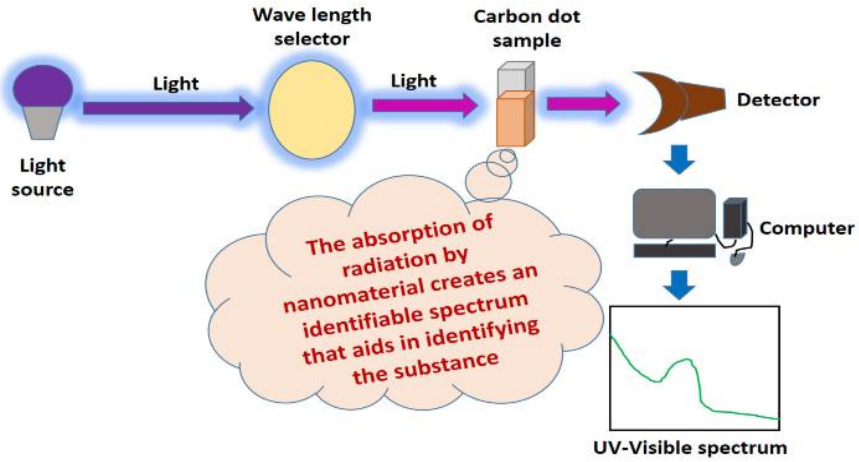


Fig. 4. Basic settings for UV-Vis spectrum measurement (Jing et al., 2023)

The UV-Vis results can be used to assess light absorption capabilities that affect photoluminescence characteristics and their potential application in photocatalysis. Based on research conducted by (Mansuriya & Altintas, 2021), Optical absorption in CQDs generally occurs in the short wavelength region due to π–π* transitions from C=C bonds in the carbon structure, with maximum intensity in the 260–320 nm range in the ultraviolet region. This absorption band is associated with π–π* transitions from aromatic $sp^2$ carbon bonds, while the shift of absorption to longer wavelengths (around 300–350 nm) is associated with n–π* transitions originating from carbonyl groups (C=O) or other functional groups containing heteroatoms.

### *3.2.3 Transmission electron microscopy*

Transmission Electron Microscopy is a characterization technique widely used in science due to its ability to display images of objects on a scale ranging from micrometers to angstroms. The working principle of TEM is based on the penetration of high-energy electron beams through very thin samples, where electrons interact with the atoms that make up the material through two types of scattering, namely elastic scattering, which stores high-resolution information, and inelastic scattering, which can cause energy loss and damage to the sample structure. The TEM instrument consists of several main components, such as an electron source, condenser lens, sample holder, objective lens, projector lens, and a detection system in the form of a screen or camera. The components found in Transmission Electron Microscopy can be seen in Figure 5 (Franken et al., 2020).

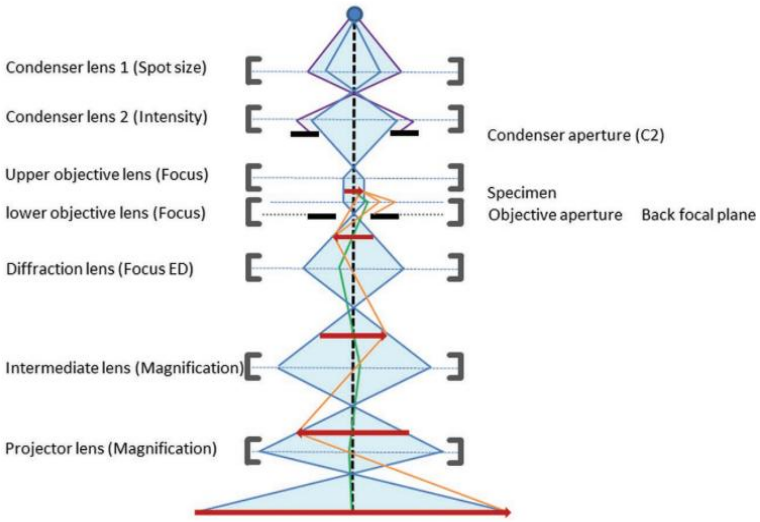


Fig. 5. Components in TEM
(Franken et al., 2020)

TEM is one of the main techniques used in CQDs characterization due to its ability to provide detailed information on morphology, particle size distribution, and crystalline structure. With a high resolution of approximately 0.2 nm, TEM produces nanometer-scale images of particles through the interaction of high-energy electron beams that penetrate the sample, thereby providing highly accurate structural information (Jing et al., 2023). The image obtained is influenced by the electron density in each part of the sample. Parts with higher density or atomic number will appear darker because they absorb or scatter more electrons, while thinner or less dense parts appear brighter because more electrons are transmitted (Ribet et al., 2021).

### *3.2.4 Fourier transformed infrared spectroscopy*

Fourier Transform Infrared Spectroscopy (FTIR) is a spectroscopic technique used to analyze surface functional groups and chemical bonds in materials, including nanomaterials

such as CQDs (Cui et al., 2021). The surface of CQDs generally consists of various functional groups such as hydroxyl, carboxyl, and epoxy or ether groups. FTIR analysis is performed by utilizing the absorption of light energy at certain frequencies, which is then measured using an infrared spectrometer as shown in Figure 6. The measurement data is displayed in the form of a spectrum that describes the relationship between the percentage of transmittance and the wave number (Jing et al., 2023).

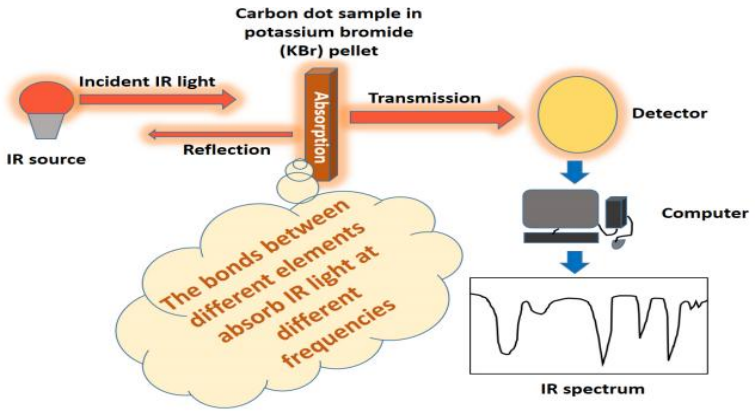


Fig. 6. Basic settings for IR spectrum measurement (Jing et al., 2023)

The characteristic absorption bands of CQDs can be identified through FTIR, such as the C=O stretching absorption band at a wavelength of 1640 $cm^{-1}$, the O-H stretching absorption band at a wavelength of 3398 $cm^{-1}$, and the C=C absorption band at a wavelength of 1415 $cm^{-1}$. The FTIR method has advantages in describing the functionalization of the CQDs surface because of its low cost, easy procedure, and quick and simple sample preparation. However, this technique is less capable of providing in-depth structural information about the carbon dots core and details of doping with heteroatom metals (Jing et al., 2023).

### *3.2.5 X-Ray diffraction*

X-Ray Diffraction (XRD) is a non-destructive analysis technique used for characterizing crystalline materials. This method provides information about crystal structure, phase, crystal orientation, grain size, crystallinity, strain, and crystal defects. The working principle of XRD is based on the constructive interference of monochromatic X-rays reflected by atomic planes in crystals. When Bragg's Law ($n\lambda = 2d \sin\theta$) is satisfied, a diffraction pattern is formed that becomes a unique fingerprint for each crystalline material (Liu et al., 2020).

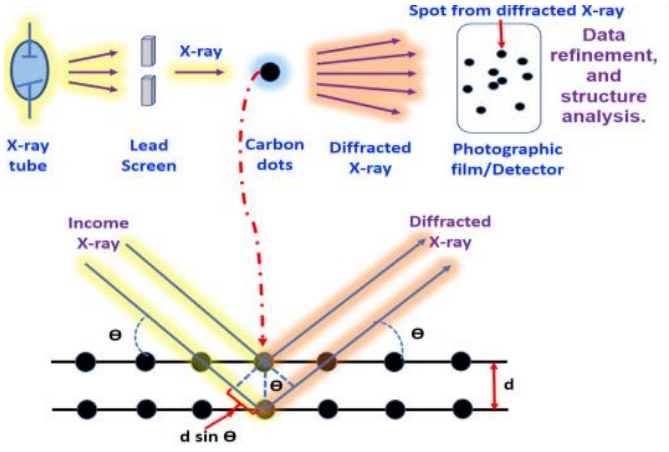


Fig. 7. Graphical demonstration of X-ray diffraction (Jing et al., 2023)

When monochromatic X-rays interact with CQDs samples, wave amplification occurs as shown in Figure 7. Exposure to X-rays causes electrons to become excited, forming a diffraction pattern that describes a regular spatial arrangement. These diffracted X-rays are then detected, processed, and calculated, yielding information about the average structure of the nanomaterial (Jing et al., 2023). Based on research conducted by (Shen et al., 2025), The results of XRD analysis of CQDs synthesized through the hydrothermal method using Solanum nigrum L. and triethylamine showed a broad diffraction peak at 2θ around 26°, indicating the presence of an amorphous or irregular carbon structure typical of graphene. This diffraction pattern indicates that CQDs have a low degree of crystallinity, which is caused by the dispersion of nitrogen atoms and the presence of oxygen functional groups on their surface.

### *3.2.6 X-ray photoelectron spectroscopy*

X-ray Photoelectron Spectroscopy or XPS is a sensitive surface analysis technique, where the working principle is that X-rays will shoot the surface of a material with high energy and measure the kinetic energy of the emitted electrons, which are then analyzed by a detector. The two main characteristics of this technique are the abundance of elements on the surface and the ability to reveal information about the elemental components of the sample. All elements except hydrogen and helium can be detected by XPS (Stevie & Donley, 2020). The resulting XPS spectrum is the sum of detected plots versus binding energy (BE) derived from the kinetic energy of the emitted photoelectrons. A schematic diagram of the XPS spectrometer and the photoemission process is shown in Figure 8.

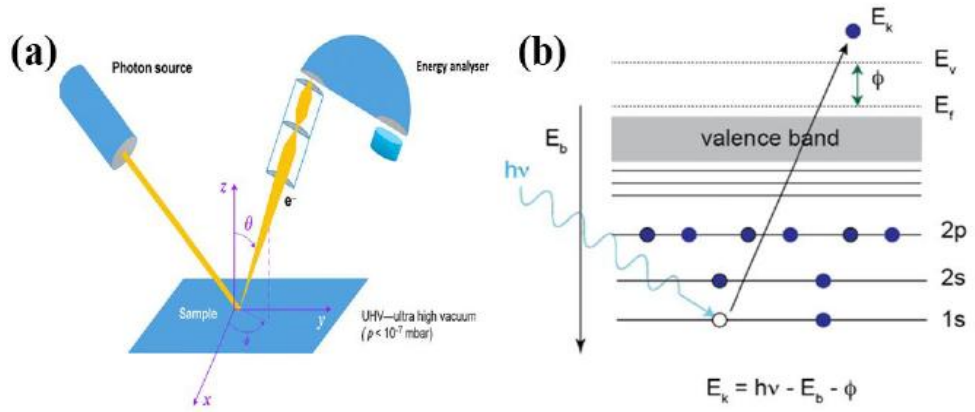


Fig. 8. (a) Schematic diagram of an XPS spectrometer, and (b) Photoemission process, copyright 2018, Elsevier (Napporn et al., 2018)

When the sample surface is irradiated with an X-ray beam of energy hν, photoelectrons with kinetic energy (KE) are emitted from the surface through the photoemission process. In a photoelectron spectrometer, the KE of the photoelectrons is measured. KE is related to the binding energy (BE) through the following equation Eq. 1. This binding energy represents the energy of electrons bound to the nucleus through the relationship given by equation 1. The term φ represents the work function of the spectrometer sample, and is a factor that depends on the instrument specified during the calibration procedure (Napporn et al., 2018).

$$h\nu = EB + EK + \varphi \quad \text{(Eq. 1)}$$

### *3.3 Bioimaging in vivo and in vitro*

Biomedical imaging has developed rapidly. Many of them conduct experiments with various types of human and animal cells. As Shukla et al. (2020), conducted research on the

synthesis of CQDs from pure sandalwood powder using an environmentally friendly hydrothermal method without additional chemicals. The resulting CQDs were 4–6 nm in size with a spherical shape and showed a UV–Vis absorption peak at 270 nm, which is characteristic of carbon aromatic groups. Bright blue fluorescence emission with a quantum yield (QY) of 12% indicates good optical efficiency. Cytotoxicity testing shows that CQDs are safe for MG-63 cells and are colloidally stable with a negative charge. Bioimaging applications show strong fluorescence in plant and animal tissues, confirming the potential of sandalwood CQDs as an environmentally friendly bioimaging agent. In addition, Karuppasamy et al. (2025b) has conducted research on the synthesis of Wood Sorrel Carbon dots (WSCQDs) using the hydrothermal method. WSCQDs are spherical in shape, measuring approximately 4–6 nm, and exhibit UV–Vis absorption peaks at 270 nm and 340 nm, which are related to π–π* and n–π* transitions. This material exhibits bright blue emission at 440 nm with QY=11.2% and a band gap energy value of 3.40 eV, demonstrating superior optical properties. The zeta potential value of −31.6 mV indicates excellent dispersion stability. Biocompatibility testing showed fibroblast cell viability of over 93% up to a concentration of 150 μg/mL, while antioxidant activity reached 79% in the DPPH assay. WSCQDs also exhibit strong fluorescence within the cell cytoplasm, making them highly promising as both bioimaging agents and environmentally friendly antioxidants.

Anpalagan et al., (2023) conducted research on CQDs from white bread, whole meal bread, and multigrain bread using the hydrothermal method for bioimaging of CT-26 (mouse) and HT-29 (human) colon cancer cells. With their extremely small particle size (average 3–7 nm), CQDs are able to penetrate cell membranes and internalize into the cytoplasm of colon cancer cells, both CT-26 (mouse) and HT-29 (human). CQDs emit clear and stable green fluorescence within cells, without disturbing cell viability, which remains above 95% even at high concentrations (1.5 mg/mL). In addition, they have green fluorescence emission properties at an emission peak of 540 nm, with a low quantum yield of around 0.03-0.81%.

Table 2. Classification of carbon dots from biomass, bioimaging objects, and CQDs characteristics

| Biomass precursor | Objects | Results |
|---|---|---|
| *Platanus* (Ren et al., 2019) | HeLa (human cervical cancer cells), L02 (normal human liver cells), and macrophage cells | a. NM-CQDs exhibit two strong and stable PL emissions at 447 nm and 476 nm (indigo–blue color).<br>b. They have a QY of 32.4% and a lifetime of 6.56 ns.<br>c. PL emissions are stable against variations in pH, temperature, and ion concentration.<br>d. Bioimaging results show good internalization and non-toxicity. |
| *Epigynum mauritum leaves* (Shi et al., 2025) | HaCaT cells (human keratinocytes) and A549 cells (human lung cancer) | a. Near-infrared emission: Emission peak at 678 nm (bright red light).<br>b. High quantum yield: 27.22% at 409 nm excitation.<br>c. Ultra-small size: 0.2–3 nm (average 1.34 ± 0.29 nm).<br>d. Cell viability >90% even at high concentrations (200 μg/mL)<br>e. Safe for vital organs (heart, brain, liver, kidneys, etc.) based on histopathological analysis.<br>f. NIR-CQDs successfully enter cells and are primarily localized in the cytoplasm. |
| Wheat straw and bamboo residues (Huang et al., 2019) | L929 fibroblast cells, SP2/0 cells, Smmc-7721 cells. | a. CQDs emit blue-green fluorescence with a quantum yield of ~13%, which is relatively high for carbon-based materials.<br>b. Fluorescence remains stable across a wide temperature range (4–60°C) and is resistant to photobleaching (only a 7–9% decrease after 90 minutes of UV irradiation), which is better than DAPI (45–50% decrease). |

| | | |
|---|---|---|
| | | c. MTT assays on L929 fibroblast cells showed cell viability >90% even at CQDs concentrations up to 400 μg/mL. |
| *Bacteri B. subtilis* (Ou et al., 2021) | Gram-positive bacteria: Bacillus subtilis, Staphylococcus aureus, Listeria monocytogenes Gram-negative bacteria: Escherichia coli, Salmonella enteritidis, Vibrio parahaemolyticus | a. N-CQDs can emit green and red fluorescence when excited at different wavelengths (490 nm and 557 nm).<br>b. 490 nm excitation → emission ~560–600 nm (green, FITC filter)<br>c. 557 nm excitation → emission ~613 nm (red, TRITC filter)<br>d. N-CQDs specifically label cell membranes and septa (walls separating cells during division) in: Gram-positive bacteria: Bacillus subtilis, Staphylococcus aureus, Listeria monocytogenes<br>e. Gram-negative bacteria: Escherichia coli, Salmonella enteritidis, Vibrio parahaemolyticus. |
| Black Fungus (Qin et al., 2021) | HeLa cell | a. The CQDs produced emit strong blue fluorescence when excited at a wavelength of 370 nm.<br>b. Cytotoxicity tests on HeLa cells show that cell viability remains above 80% even at high CQDs concentrations (800 μg/mL) after 48 hours.<br>c. CQDs were successfully used for in vitro fluorescence imaging of HeLa cells. After incubation with CQDs for 4 hours, the cells showed a clear blue fluorescence signal under a fluorescence microscope. |
| *Chestnut dan peanuts* (Mancini et al. 2023) | BALB/3T3 fibroblast cells. | a. CQDs are not cytotoxic to BALB/3T3 fibroblasts.<br>b. Blue fluorescence signals are detected using a DAPI filter (λem = 420 nm).<br>c. Cell viability is >95% even at high concentrations (0.5 μg/μL) after 24 hours of incubation.<br>d. Useful for monitoring biological processes such as cell proliferation, apoptosis, and tumor growth. |
| Lemon juice (Zhang et al., 2023) | HeLa Cell | a. CQDs are on average 2.9 nm in size, spherical in shape with a graphite structure (lattice spacing 0.21 nm).<br>b. They have a high Quantum Yield (QY) of 58.66%, strong blue fluorescence, and are stable against pH, light, and ions.<br>c. They exhibit excellent photoluminescence stability and resistance to quenching.<br>d. Can selectively and sensitively detect $Fe^{2+}$ ions with a linear range of 2–625 μM and a detection limit of 0.063 μM.<br>e. MTT assay shows HeLa cell viability >95%, indicating high biocompatibility.<br>f. Effective for multicolor bioimaging (blue and green) in HeLa cells. |
| *Passion fruit (Passiflora edulis Sims)* (Wang et al., 2020) | Fibroblast cells | a. N-QDs have an average size of 3.8 nm and a uniform shape with a thickness of 0.7–1.2 nm. |

| | | |
|---|---|---|
| | | b. They exhibit strong, multicolor fluorescence (blue, green, yellow) that can be controlled through reaction time and temperature.<br>c. They have a Quantum Yield (QY) of 29% and high photoluminescence stability against pH, light, and ions. Fibroblast cell viability remains high (non-toxic) up to a concentration of 500 µg/mL.<br>d. Effective for multicolor bioimaging and $Ag^+$ ion fluorescent sensors with a detection limit of 1.2 nM. |
| Mushroom fiber (Shi et al., 2019) | HepG2 cells (human liver cells) | a. N,S-CQDs measuring 2–5 nm with uniform distribution.<br>b. Display excitation-dependent fluorescence, with blue–green–red emission depending on wavelength.<br>c. High fluorescence stability and no significant quenching.<br>d. Cell viability >95% at concentrations up to 400 µg/mL, demonstrating biocompatibility and non-toxicity.<br>e. Effective for multicolor bioimaging in HepG2 cells.<br>f. Can also be used for detection of tetracycline antibiotics (TC, CTC, OTC) with a recovery rate of 90–110%. |
| Banana peel (Atchudan et al. 2018) | Nematodes | a. CQDs are not only bound to cell membranes, but also enter all parts of the nematode's body.<br>b. High Biocompatibility: Toxicity tests on nematodes show no significant decrease in viability even at a concentration of 200 µg/mL.<br>c. Can emit different colors (blue, green, red) depending on the excitation wavelength.<br>d. Quantum yield (QY): 20% – relatively high for natural CQDs without passivation.<br>e. Size: Average 5 nm with a narrow size distribution (4–6 nm). |
| *Bermuda grass (Cynodon dactylon)* (Gurung et al., 2023) | HeLa cancer cells and normal L929 cells | a. CQDs measuring 2–6 nm, amorphous spherical in shape with uniform dispersion.<br>b. Exhibits bright blue fluorescence under UV light, with maximum emission at 440 nm upon excitation at 360 nm.<br>c. Quantum Yield 17.3% and high PL stability against pH, ions, and storage time.<br>d. MTT assay shows cell viability >90% up to a concentration of 500 µg/mL.<br>e. Effective for bioimaging HeLa and L929 cells with strong fluorescence without significant toxicity. |
| *Chenopodium album leaves (Bathua vegetable plant)* (Kansay et al., 2023) | SH-SY5Y cells (neuroblastoma), HCT-116 cells (colon cancer), fungi, bacteria, pine needles, and | a. N,K,Ca-CQDs with an average size of 3–5 nm, almost spherical in shape and polycrystalline in nature.<br>b. Quantum Yield 48.12%, bright yellow-green fluorescence with high stability and good solubility in water. |

| | | |
|---|---|---|
| | button mushrooms | c. High PL stability, sensitive to pH and solvents but still showing stable emission (454–453 nm).<br>d. Cell viability >95% for SH-SY5Y and HCT-116 at 200 µg/mL; other organisms can survive up to 10.9 mg/mL for 4 days.<br>e. Effective for bioimaging cancer cells and living organisms, producing strong green fluorescence without significant toxicity. |
| *Holly leaves* (Hu et al., 2024) | Cancer cells (HepG2, HeLa, T24), Liver cells (7702). | a. Red (near-infrared) fluorescence emission with an emission peak at 684 nm.<br>b. Particle size: 2.0–4.5 nm (average 3.5 nm), spherical and evenly distributed.<br>c. High stability: no photobleaching for 6 months, stable against pH and NaCl concentration variations.<br>d. Quantum yield (QY): 19.88%.<br>e. Cytotoxicity testing on HepG2 cells showed cell viability >90% even at RCQDs concentrations up to 300 µg/mL.<br>f. RCQDs successfully entered four types of cells: HepG2 (liver cancer), HL-7702 (normal liver cells), T24 (bladder cancer), and HeLa (cervical cancer). |
| *Mexican mint leaf extract (Plectranthus amboinicus)* (Architha et al., 2021) | HeLa cells and L929 cells | a. CQDs measuring 4–7 nm, amorphous spherical in shape with uniform dispersion.<br>b. Exhibits strong blue fluorescence with a maximum emission of 440 nm.<br>c. Quantum Yield 21.7%, stable against pH, metal ions, and storage time.<br>d. MTT assay shows cell viability >95% up to a concentration of 500 µg/mL, indicating high biocompatibility.<br>e. Effective for multicolor bioimaging in HeLa and L929 cells without significant toxicity. |
| *Raw black mulberry fruit (Morus nigra)* (Atchudan et al., 2025) | Fibroblast cells, human mesenchymal stem cells (HMSCs), and macrophage cells | a. ME-CQDs measuring 2–6 nm, partially amorphous with a graphitic structure.<br>b. Exhibits excitation-dependent emission (400–533 nm) with a quantum yield of 24%.<br>c. Stable for 200 days and resistant to 150 minutes of UV irradiation (without photobleaching).<br>d. Cell viability > 98% up to 100 µg/mL in fibroblasts, HMSCs, and macrophages.<br>e. Effective for 2D and 3D bioimaging and cell migration, and functions as a stable anti-counterfeit fluorescent ink for up to 150 days. |
| Ginkgo biloba seeds (Zhang et al., 2022) | HeLa cells | a. CQDs are 2–5 nm in size, nearly spherical in shape, and well dispersed.<br>b. They exhibit bright blue fluorescence with a maximum emission of 450 nm and a quantum yield of 19.6%.<br>c. Stable to pH 3–11, light, and metal ions.<br>d. Possess –OH, –COOH, and $–NH_2$ functional groups that enhance water solubility.<br>e. HeLa cell viability > 95% up to a concentration of 500 µg/mL, indicating high biocompatibility.<br>f. Effective for multicolor (blue–green) bioimaging in HeLa cells without toxicity. |
| Manilkara zapota fruits (Bhamore et al., 2019) | Bacterial cells and fungal cells | a. C-dots have been successfully used for imaging bacterial cells (E. coli) and fungal cells (Aspergillus aculeatus and Fomitopsis sp.).<br>b. They can emit blue, green, and red colors depending on the excitation wavelength (405, 488, 561 nm). |

| | | |
|---|---|---|
| | | c. Cytotoxicity testing on HeLa cells showed no toxicity up to a concentration of 300 μg/mL, proving high biocompatibility.<br>d. Multi-colored C-dots from Manilkara zapota fruit are effective and safe fluorescent agents for microbial cell bioimaging. |
| Orange juice (Kasirajan et al., 2024) | MCF-7 breast cancer cells | a. CQDs measuring 2–6 nm, spherical in shape with a graphitic structure (d-spacing 0.21 nm).<br>b. Exhibits bright green emission (515 nm) with excitation at 420 nm and a quantum yield of 4.1%.<br>c. Stable at pH 2–9, light, and storage.<br>d. Selective for $Fe^{3+}$ with a detection limit of 0.7 μM and linearity of 0–100 μM.<br>e. Shows strong antibacterial activity against S. aureus and K. pneumoniae and inhibits biofilm formation by up to 91%.<br>f. MCF-7 cell viability >90% up to 50 μg/mL and still 81% at 100 μg/mL.<br>g. Effective for multicolor bioimaging (blue–green–red) without significant toxicity. |
| *Pistachio shells (PS) and peanut shells (GNS)* (Manjubaashini et al., 2024a) | Fibroblast cells & zebrafish embryos (Zebrafish larvae) | a. Spherical morphology with particle sizes of ± 4.5–5 nm (PSE) and ± 10–14 nm (GNSE).<br>b. Amorphous structure with interlayer spacing of 0.33 nm (PSE) and 0.32 nm (GNSE).<br>c. UV–Vis spectrum shows absorption at 240–242 nm (π–π*) and 370/309 nm (n–π*).<br>d. Fluorescence emission: 456 nm (PSE, blue) and 440 nm (GNSE, green).<br>e. Quantum yield: 9.5% (PSE) and 9.0% (GNSE).<br>f. Zeta potential: +0.04 mV (PSE) and −0.02 mV (GNSE).<br>g. Fibroblast cell viability >95% up to a concentration of 100 μL.<br>h. High hemocompatibility with hemolysis of 0.3% (PSE) and 0.1% (GNSE).<br>i. Able to penetrate zebrafish embryo tissue and produce strong fluorescence in the yolk sac and eye areas. |
| White rise waste (Anthony et al., 2020) | A549 cells (Human lung cancer) | a. r-CQDs-GS has a Quantum Yield (QY) = 41%.<br>b. Emits very bright blue fluorescence under UV light (365 nm), with peak emission at 432 nm when excited at 340 nm.<br>c. Cytotoxicity testing with the MTT assay on A549 cells (human lung cancer) showed cell viability >90% even at high concentrations (100 μg/mL).<br>d. After incubation with A549 cells for 1 hour, r-CQDs-GS successfully entered the cells and emitted a strong green fluorescence signal when observed under a fluorescence microscope (488 nm). |

### *3.4 Biomedical application*

CQDs from biomass have attracted the attention of researchers due to their sustainability, low cost, ease of synthesis, tunable optical properties, and superior biocompatibility. This class of green nanomaterials is very promising and has great potential in the medical field, especially in bioimaging applications, both in vivo and in vitro. Figure 9(a) shows quaternized CQDs and its potential in selective bioimaging of gram-positive bacteria, and 9(b) shows the ability of multicolor CQDs for imaging in live animal studies. In vivo mouse-based CQDs bioimaging as an intravenous fluorescent dye;

Illustration of dissected animal organs 24 hours after intravenous administration of CQDs solution.

Biomass as a precursor not only minimizes environmental impact and provides heteroatoms and natural functional groups, but also offers fluorescence-based and surface reactivity, making this class of nanomaterials highly promising in the biomedical and biological systems fields. In collagenase inhibition activity, CQDs serves as an inhibitor of aging activity, a skin care formulation to maintain health, and helps collagen, skin structural integrity, and tissue rejuvenation (Chen et al., 2021; Hua et al., 2021; Wang et al., 2025). Additionally, in DNA protection studies, preliminary studies have shown that CQDs has antioxidant properties and can protect DNA from oxidative damage by neutralizing ROS (Wang et al., 2025; Yao et al., 2023). In vivo studies on Coccinia Grandis showed that CQDs had excellent absorption and the ability to emit light in various colors, including blue, green, and red, which was achieved by adjusting the excitation wavelength and its resistance to photobleaching (Karuppasamy et al., 2024).

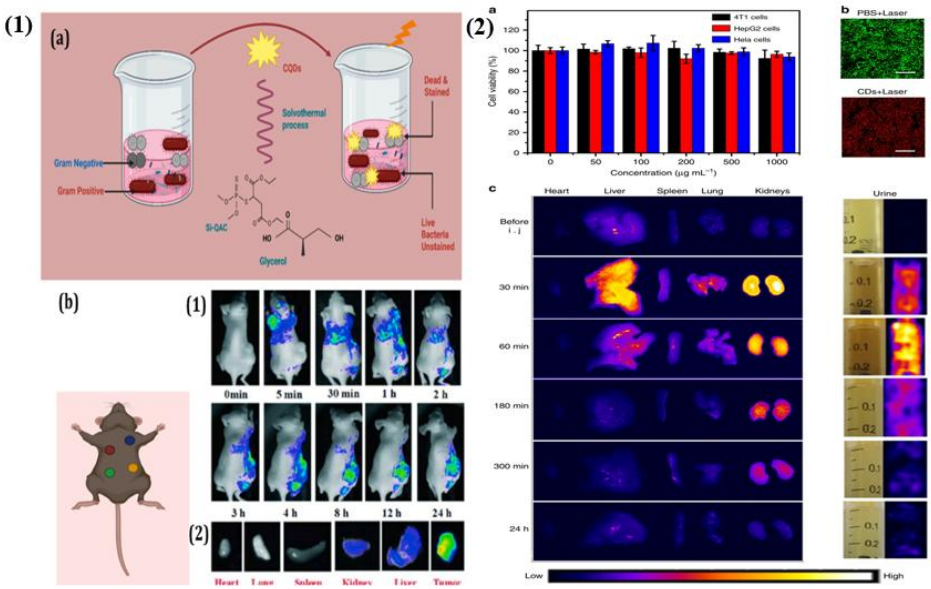


Fig. 9. (1) parts (a) Quaternized CQDs and its potential in selective bioimaging of gram-positive bacteria, and (b) shows the ability of multicolor CQDs for imaging in live animal studies. (1) In vivo mouse-based CQDs bioimaging as an intravenous fluorescent dye; (2) Illustration of dissected animal organs 24 hours after intravenous administration of CQDs solution. Hak cipta 2024, Elsevier (Salvi et al., 2024) and for (2) parts (a) Relative cell viability of HeLa cells at various concentrations (0–1000 μg $mL^{-1}$) after 24 hours of incubation with CQDs. (b) Confocal fluorescence image of HeLa cells incubated in PBS solution and aqueous CQDs solution (200 μg $mL^{-1}$) after irradiation with a 655 nm laser at 1 W $cm^{-2}$ for 10 minutes; scale bar: 200 μm. (c) NIR fluorescence of major organs dissected from mice without and with intravenous injection of aqueous CQDs solution (0.2 mL, 1000 μg $mL^{-1}$) after various time points (left) and bright field and NIR fluorescence images of urine collected at the corresponding time points (right). NIR fluorescence images were obtained using the Fluor Vivo Model-300 in vivo optical imaging system with xenon lamp excitation. The excitation wavelength was 639–713 nm and the fluorescence collection channel was 714–780 nm.
(Bao et al., 2018).

In vivo studies using CQDs-based materials in bioimaging applications have shown the absorption capabilities and toxicity of CQDs, and have utilized CQDs as a highly efficient means of mimicking the human anatomical genome. Additionally, the CQDs from biomass will be highly bioactive, absorbent, biodegradable, and contain active chemical compounds for productive biological screening. Rarely, PS-derived CQDs and GNS are combined for

complex direct imaging applications (from cellular to organ level) (Manjubaashini et al., 2024b). As is known, different cell types have different structures and morphologies, and different cell membranes or cytoplasms contain different biomarkers, leading to specific responses to foreign nanoparticles. Based on this, CQDs with special functions were synthesized and used in biological imaging technology, which also provides the possibility of applying CQDs in in vitro bioimaging, which is expected to promote the development of cell imaging techniques (He et al., 2022). Based on previous studies, CQDs S, doped with N, exhibits strong absorption bands in the red to NIR region of citric acid, urea, and DMSO via the solvothermal method. In this method, DMSO serves as both the solvent and the source of S doping. Under 655 nm laser irradiation, the aqueous CQDs solution exhibits NIR fluorescence (centered at 720 nm) and high photothermal conversion efficiency (η = 59.2%). The prepared CQDs was excreted via the kidneys in vivo and showed very low cytotoxicity. After intravenous administration, CQDs accumulates in tumor tissue and exhibits strong PA signals and NIR fluorescence. More importantly, tumors are eradicated after intravenous injection of CQDs (1 mg mL^(−1), 200 μL) followed by irradiation with a 655 nm laser (1 W cm^(−2) for 5 min) (Bao et al., 2018).

In vitro studies show tunable emission responses, with QY increasing to 42.72% and maintaining normal morphology (Murugan et al., 2024). In vitro studies in previous research, such as the use of FP-CQDs-βCyD material, showed a similar response to pH as FP-CQDs, indicating that the presence of cyclodextrin groups does not alter its ability to recognize H+ ions thru the PET process. This demonstrates biocompatibility with cell lines, reduces cell viability, and induces changes in cell cycle phase distribution (Espina-Casado et al., 2021a; Espina-Casado et al., 2021b). Additionally, other researchers conducted in vitro studies using HeLa and RAW 264.7 cells, leading to new findings where cell viability showed that surface conjugation with NH2-CQD not only improved the cytocompatibility of TO-CNC but also enhanced cellular association and internalization in HeLa and RAW 264.7 cells after 4 and 24 hours of incubation (Guo et al., 2017). Based on previous in vitro studies, the results of in vitro ACE2 quantification, where increasing CQDs concentrations (75 ppm, 150 ppm, 300 ppm) caused an increase in ACE2 activity or expression, were displayed in arbitrary units (a.u.). In addition, molecular interactions occurred between the functional atoms of CQDs and the active site of ACE2 (Mailisa et al., 2023).

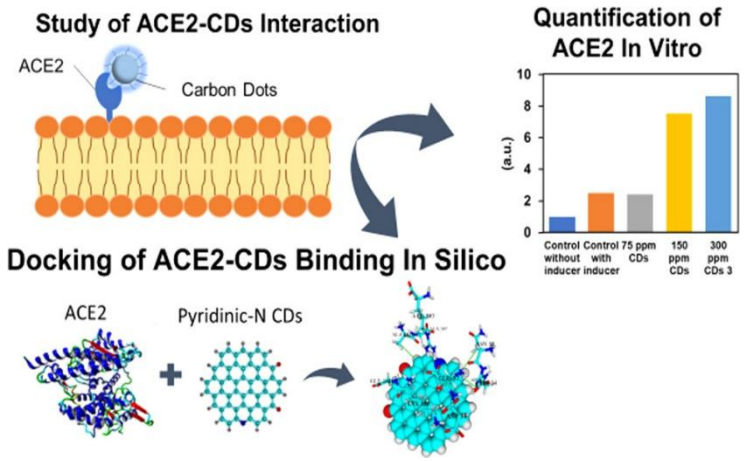


Fig. 10. Schematic illustration of the interaction between ACE2 and pyridinic-N doped carbon dots (N-CQDs). In silico docking demonstrates the potential binding between ACE2 and N-CQDs through non-covalent interactions. The bar graph on the right shows in vitro quantification of ACE2, indicating increased activity with higher CQDs concentrations (Mailisa et al., 2023).

Overall, CQDs from biomass in bioimaging is a sustainable and environmentally friendly approach. CQDs is a biocompatible carbon material for developing modern healthcare technology. In vitro and in vivo bioimaging as two fluorescence-based imaging

techniques. Continuous optimization of their synthesis, functionalization, and photophysical properties will be key to fully realizing their potential in future clinical applications.

## 4. Conclusions

Biomass-derived CQDs have emerged as sustainable, biocompatible, and multifunctional nanomaterials with remarkable potential in both in vitro and in vivo bioimaging. The utilization of renewable biomass precursors offers an eco-friendly and cost-effective route to synthesize fluorescent nanoprobes with excellent water solubility, tunable emission, and low cytotoxicity. The small particle size (typically 2–10 nm) and rich surface functionalities, such as hydroxyl, carboxyl, and amino groups, enable efficient cellular uptake and stable fluorescence within biological environments. In in vitro systems, biomass-based CQDs exhibit strong and stable multicolor fluorescence, allowing precise imaging of various cell types with cell viability generally exceeding 85–95% even at high concentrations. In in vivo studies, these nanomaterials demonstrate favorable biodistribution, rapid clearance, and minimal toxicity in animal models such as zebrafish and mice, confirming their safety and compatibility for real-time tissue imaging. Some CQDs further display near-infrared (NIR) emission, facilitating deep-tissue visualization and reducing background autofluorescence. Beyond imaging, many biomass-derived CQDs possess intrinsic antioxidant, antibacterial, and sensing capabilities, positioning them as versatile candidates for integrated biomedical applications such as diagnosis, therapy, and biosensing. Overall, the convergence of sustainability, optical performance, and biocompatibility underscores biomass-derived CQDs as next-generation green nanoprobes for future clinical and diagnostic bioimaging platforms.

## Acknowledgement
The author would like to thank the institutions whose data was used to facilitate this research. Author also thankfully to EPA composting/MSW facts, BMUV/EEA country factsheets, DEFRA/Local authority collected waste, Swedish waste management report, MOE Japan food loss & waste and total waste, National waste & resource recovery report 2024, and National Waste Report 2022 for providing data of biomass waste.

## Author Contribution
Writing – Review & Editing, Writing – Original Draft Preparation, Conceptualization, Visualization, Investigation, Validation, Methodology, Resources.

## Funding
No funding of this research.

## Ethical Review Board Statement
Not available.

## Informed Consent Statement
Not available.

## Data Availability Statement
All data reported in this paper are derived from publicly available sources, including characterization data, procedures, methods, and animal use. No new data is created or unavailable due to privacy or ethical restrictions.

## Conflicts of Interest
The author declares no conflict of interest.

## References

Ahn, J., Pealer, C., & Kim, S. (2024). Analysis of Carbon Dots Synthesized at Different Hydrothermal Carbonization Temperatures and Their Ferric Ion Detection Performances. *Physica Status Solidi (b)*, *261*(7). https://doi.org/10.1002/pssb.202300345

Alhussaini, M. S., Alyahya, A. R. A. I., & Al-Ghanayem, A. A. (2026). Recent progress in quantum dots for antimicrobial therapy and bioimaging: A comprehensive review (2018 to mid-2025). *Dyes and Pigments*, *245*, 113294. https://doi.org/10.1016/J.DYEPIG.2025.113294

Altaylı, B., Toprak, Y. E., Çubuk, S., Uyumaz, F., & Kahraman, M. V. (2025). Fluorescent carbon quantum dots for toxic Mercury (II) ions detection in environmental waters. *Surfaces and Interfaces*, *74*, 107668. https://doi.org/10.1016/J.SURFIN.2025.107668

Amloy, S., Lukprang, T., Lertworapreecha, M., & Preechaburana, P. (2024). Green synthesis of carbon dots from mangosteen peel for fluorescent cancer cells. *Journal of Metals, Materials and Minerals*, *34*(2), 1957. https://doi.org/10.55713/jmmm.v34i2.1957

Anpalagan, K., Karakkat, J. V., Jelinek, R., Kadamannil, N. N., Zhang, T., Cole, I., Nurgali, K., Yin, H., & Lai, D. T. H. (2023). A Green Synthesis Route to Derive Carbon Quantum Dots for Bioimaging Cancer Cells. *Nanomaterials*, *13*(14). https://doi.org/10.3390/nano13142103

Anthony, A. M., Murugan, R., Subramanian, R., Selvarangan, G. K., Pandurangan, P., Dhanasekaran, A., & Sohrab, A. (2020). Ultra-radiant photoluminescence of glutathione rigidified reduced carbon quantum dots (r-CQDs) derived from ice-biryani for in vitro and in vivo bioimaging applications. *Colloids and Surfaces A: Physicochemical and Engineering Aspects*, *586*. https://doi.org/10.1016/j.colsurfa.2019.124266

Architha, N., Ragupathi, M., Shobana, C., Selvankumar, T., Kumar, P., Lee, Y. S., & Kalai Selvan, R. (2021). Microwave-assisted green synthesis of fluorescent carbon quantum dots from Mexican Mint extract for Fe3+ detection and bio-imaging applications. *Environmental Research*, *199*(May), 111263. https://doi.org/10.1016/j.envres.2021.111263

Ashraf, H., & Karahan, B. D. (2024). Biowaste valorization into valuable nanomaterials: Synthesis of green carbon nanodots and anode material for lithium-ion batteries from watermelon seeds. *Materials Research Bulletin*, *169*, 112492. https://doi.org/10.1016/j.materresbull.2023.112492

Atchudan, R., Edison, T. N. J. I., Aseer, K. R., Perumal, S., & Lee, Y. R. (2018). Hydrothermal conversion of Magnolia liliiflora into nitrogen-doped carbon dots as an effective turn-off fluorescence sensing, multi-colour cell imaging and fluorescent ink. *Colloids and Surfaces B: Biointerfaces*, *169*, 321–328. https://doi.org/10.1016/j.colsurfb.2018.05.032

Atchudan, R., Edison, T. N. J. I., Perumal, S., Vinodh, R., Sundramoorthy, A. K., Babu, R. S., & Lee, Y. R. (2021). Leftover Kiwi Fruit Peel-Derived Carbon Dots as a Highly Selective Fluorescent Sensor for Detection of Ferric Ion. *Chemosensors*, *9*(7), 166. https://doi.org/10.3390/chemosensors9070166

Atchudan, R., Karuppasamy, B. D., Perumal, S., Gangadaran, P., Sundramoorthy, A. K., Manoj, D., Rajendran, R. L., Ahn, B. C., Ahamed, M., Lee, S. W., & Lee, Y. R. (2025). Sustainable-biomass-derived multifunctional carbon dots as fluorescent probes for multi-purpose advanced imaging, migration and security solutions. *Surfaces and Interfaces*, *62*(March). https://doi.org/10.1016/j.surfin.2025.106238

Bao, X., Yuan, Y., Chen, J., Zhang, B., Li, D., Zhou, D., Jing, P., Xu, G., Wang, Y., Holá, K., Shen, D., Wu, C., Song, L., Liu, C., Zbořil, R., & Qu, S. (2018). In vivo theranostics with near-infrared-emitting carbon dots—highly efficient photothermal therapy based on passive targeting after intravenous administration. *Light: Science & Applications*, *7*(1), 91. https://doi.org/10.1038/s41377-018-0090-1

Basha, Z. W., Muniraj, S., & Kumar, A. S. (2024). Neem biomass derived carbon quantum dots synthesized via one step ultrasonification method for ecofriendly methylene blue dye removal. *Scientific Reports*, *14*(1), 9706. https://doi.org/10.1038/s41598-024-59483-9

Bhamore, J. R., Jha, S., Park, T. J., & Kailasa, S. K. (2019). Green synthesis of multi-color emissive carbon dots from Manilkara zapota fruits for bioimaging of bacterial and fungal cells. *Journal of Photochemistry and Photobiology B: Biology*, *191*, 150–155. https://doi.org/10.1016/j.jphotobiol.2018.12.023

Bian, J., Wang, Z., Ge, J., Gong, W., Nan, K., Liu, Z., Guo, J., Zhao, Q., Wang, X., & Wan, L. (2025). Recent advances of fluorescent carbon dots for biological imaging and biosensing. *Chemical Engineering Journal*, *519*, 165135. https://doi.org/10.1016/J.CEJ.2025.165135

Cai, D., Zhong, X., Xu, L., Xiong, Y., Deng, W., Zou, G., Hou, H., & Ji, X. (2025). Biomass-derived carbon dots: synthesis, modification and application in batteries. *Chemical Science*, *16*(12), 4937–4970. https://doi.org/10.1039/D4SC08659G

Chávez-García, D., Guzman, M., Sanchez, V., & Cadena-Nava, R. D. (2024). Green synthesis of biomass-derived carbon quantum dots for photocatalytic degradation of methylene blue. *Beilstein Journal of Nanotechnology*, *15*, 755–766. https://doi.org/10.3762/bjnano.15.63

Chen, D., Li, B., Lei, T., Na, D., Nie, M., Yang, Y., Congjia, Xie, He, Z., & Wang, J. (2021). Selective mediation of ovarian cancer SKOV3 cells death by pristine carbon quantum dots/Cu2O composite through targeting matrix metalloproteinases, angiogenic cytokines and cytoskeleton. *Journal of Nanobiotechnology*, *19*(1), 68. https://doi.org/10.1186/s12951-021-00813-8

Chen, D., Zia, M. U., Yang, F., Wang, Y., Leusch, F. D. L., Nguyen, N.-T., Zhang, W., Gao, Y., Zhao, D., Raston, C. L., & Li, Q. (2023). Ligand Mediated, Spatially Confined Carbonization of Biomass Forming High-Performance Colloidal Carbon Dots. *ACS Sustainable Chemistry & Engineering*, *11*(32), 11756–11768. https://doi.org/10.1021/acssuschemeng.3c00371

Chen, J., Li, T., Lin, C., Hou, Y., Cheng, S., & Gao, B. (2025a). Green synthesis of red-emitting carbon dots for bioimaging, sensing, and antibacterial applications. *Spectrochimica Acta Part A: Molecular and Biomolecular Spectroscopy*, *328*, 125458. https://doi.org/10.1016/J.SAA.2024.125458

Chen, J., Li, T., Lin, C., Hou, Y., Cheng, S., & Gao, B. (2025b). Green synthesis of red-emitting carbon dots for bioimaging, sensing, and antibacterial applications. *Spectrochimica Acta Part A: Molecular and Biomolecular Spectroscopy*, *328*, 125458. https://doi.org/10.1016/j.saa.2024.125458

Chen, M., Zhai, J., An, Y., Li, Y., Zheng, Y., Tian, H., Shi, R., He, X., Liu, C., & Lin, X. (2022). Solvent-Free Pyrolysis Strategy for the Preparation of Biomass Carbon Dots for the Selective Detection of Fe3+ Ions. *Frontiers in Chemistry*, *10*. https://doi.org/10.3389/fchem.2022.940398

Cui, L., Ren, X., Sun, M., Liu, H., & Xia, L. (2021). Carbon Dots: Synthesis, Properties and Applications. *Gongneng Cailiao/Journal of Functional Materials*, *52*(1), 01053–01063. https://doi.org/10.3969/j.issn.1001-9731.2021.01.009

Das, S., Mondal, S., & Ghosh, D. (2024). Carbon quantum dots in bioimaging and biomedicines. *Frontiers in Bioengineering and Biotechnology*, *11*. https://doi.org/10.3389/fbioe.2023.1333752

Duan, H., Wang, Y., Zhang, Z., Akram, A., Chen, L., & Li, J. (2024). The Preparation of Biomass-Derived Carbon Dots and Its Application Prospect in the Field of Vascular Stent Coating. *Coatings*, *14*(11), 1432. https://doi.org/10.3390/coatings14111432

Eskalen, H., Uruş, S., Kavgacı, M., Kalmış, H. V., & Tahta, B. (2024). Carbon quantum dots derived from pomegranate peel: highly effective Fe(III) sensor. *Biomass Conversion and Biorefinery*, *14*(1), 1201–1214. https://doi.org/10.1007/s13399-023-04048-5

Espina-Casado, J., Fernández-González, A., Díaz-García, M. E., & Badía-Laíño, R. (2021a). Smart carbon dots as chemosensor for control of water contamination in organic media. *Sensors and Actuators B: Chemical*, *329*, 129262. https://doi.org/10.1016/j.snb.2020.129262

Espina-Casado, J., Fontanil, T., Fernández-González, A., Cal, S., Obaya, Á. J., Díaz-García, M. E., & Badía-Laíño, R. (2021b). Carbon dots as multifunctional platform for intracellular pH sensing and bioimaging. In vitro and in vivo studies. *Sensors and Actuators B: Chemical*, *346*, 130555. https://doi.org/10.1016/J.SNB.2021.130555

Fan, K., Tang, R., & Li, L. (2025). Carbon dots-melatonin-chitosan coating to alleviate chilling injury, enhance storage quality and antioxidant capacity of yellow peaches. *Food Packaging and Shelf Life*, *52*, 101629. https://doi.org/10.1016/J.FPSL.2025.101629

Fang, M., Wang, B., Qu, X., Li, S., Huang, J., Li, J., Lu, S., & Zhou, N. (2024). State-of-the-art of biomass-derived carbon dots: Preparation, properties, and applications. *Chinese Chemical Letters*, *35*(1), 108423. https://doi.org/10.1016/j.cclet.2023.108423

Feng, Z., Adolfsson, K. H., Xu, Y., Fang, H., Hakkarainen, M., & Wu, M. (2021). Carbon dot/polymer nanocomposites: From green synthesis to energy, environmental and biomedical applications. *Sustainable Materials and Technologies*, *29*, e00304. https://doi.org/10.1016/J.SUSMAT.2021.E00304

Franken, L. E., Grünewald, K., Boekema, E. J., & Stuart, M. C. A. (2020). A Technical Introduction to Transmission Electron Microscopy for Soft-Matter: Imaging, Possibilities, Choices, and Technical Developments. *Small*, *16*(14). https://doi.org/10.1002/smll.201906198

Gao, Y., Sun, T., Wu, T., Xu, J., Zhu, Y., Hu, J., Yang, H., Xu, H., Kan, Y., & Zhao, L. (2025). Microwave-assisted hydrothermal synthesis of nitrogen-rich biomass carbon dots (CDs): B, N co-doped with enhanced luminescence and dual mode afterglow emitting properties. *Carbon*, *244*, 120670. https://doi.org/10.1016/J.CARBON.2025.120670

Gedda, G., Sankaranarayanan, S. A., Putta, C. L., Gudimella, K. K., Rengan, A. K., & Girma, W. M. (2023). Green synthesis of multi-functional carbon dots from medicinal plant leaves for antimicrobial, antioxidant, and bioimaging applications. *Scientific Reports*, *13*(1), 6371. https://doi.org/10.1038/s41598-023-33652-8

Guo, J., Liu, D., Filpponen, I., Johansson, L. S., Malho, J. M., Quraishi, S., Liebner, F., Santos, H. A., & Rojas, O. J. (2017). Photoluminescent Hybrids of Cellulose Nanocrystals and Carbon Quantum Dots as Cytocompatible Probes for in Vitro Bioimaging. *Biomacromolecules*, *18*(7), 2045–2055. https://doi.org/10.1021/ACS.BIOMAC.7B00306

Guo, Y., Lu, J., Wang, W., Jiang, H., Ma, G., Han, P., & Tian, L. (2025). Molecularly imprinted polymer electrochemiluminescence sensor based on biomass carbon quantum dots from cantaloupe peel for ultrasensitive and specific detection of methylene blue. *Journal of Food Composition and Analysis*, *148*, 108363. https://doi.org/10.1016/J.JFCA.2025.108363

Gurung, S., Neha, Arun, N., Joshi, M., Jaiswal, T., Pathak, A. P., Das, P., Singh, A. K., Tripathi, A., & Tiwari, A. (2023). Dual metal ion (Fe3+ and As3+) sensing and cell bioimaging using fluorescent carbon quantum dots synthesised from Cynodon dactylon. *Chemosphere*, *339*(April), 139638. https://doi.org/10.1016/j.chemosphere.2023.139638

Haleem, A., Javaid, M., Singh, R. P., Rab, S., & Suman, R. (2023). Applications of nanotechnology in medical field: a brief review. *Global Health Journal*, *7*(2), 70–77. https://doi.org/10.1016/j.glohj.2023.02.008

He, C., Lin, X., Mei, Y., Luo, Y., Yang, M., Kuang, Y., Yi, X., Zeng, W., Huang, Q., & Zhong, B. (2022). Recent Advances in Carbon Dots for In Vitro/Vivo Fluorescent Bioimaging: A Mini-Review. *Frontiers in Chemistry*, *10*. https://doi.org/10.3389/fchem.2022.905475

Hota, N. P., & Iyer, S. K. (2024). N-doped carbon quantum dots for the selective detection of OCl− ions, bioimaging, and the production of Fe3O4 nanoparticles utilized in the synthesis of substituted imidazole. *RSC Advances*, *14*(48), 35448–35459. https://doi.org/10.1039/D4RA06474G

Hu, Y., Chen, Y., Wei, W., & Liu, H. (2024). Preparation of biomass-derived red emission carbon dots for real-time and long-term tracking of cells and tumor growth. *RSC Advances*, *14*(50), 37104–37113. https://doi.org/10.1039/d4ra05018e

Hua, Y., Zhou, L., Yang, W., An, W., Kou, X., Ren, J., Su, H., Chen, R., Zhang, Z., Zou, J., & Zhao, Z. (2021). Y-2 reduces oxidative stress and inflammation and improves neurological function of collagenase-induced intracerebral hemorrhage rats. *European Journal of Pharmacology*, *910*, 174507. https://doi.org/10.1016/j.ejphar.2021.174507

Huang, C., Dong, H., Su, Y., Wu, Y., Narron, R., & Yong, Q. (2019). Synthesis of carbon quantum dot nanoparticles derived from byproducts in bio-refinery process for cell imaging and in vivo bioimaging. *Nanomaterials*, *9*(3). https://doi.org/10.3390/nano9030387

Huang, K., Fu, J., Cai, J., Ma, G., Luo, J., & Wang, X. (2025). Advances in biomass-based carbon dots for smart food packaging applications. *Trends in Food Science & Technology*, *165*, 105298. https://doi.org/10.1016/J.TIFS.2025.105298

Huang, X., Liu, J., Zhao, B., Bai, Y., Peng, Z., Zhou, J., Wang, C., Zhao, X., Han, S., & Zhang, C. (2022). One-step Synthesis of Biomass-Based Carbon Dots for Detection of Metal Ions and Cell Imaging. *Frontiers in Energy Research*, *10*. https://doi.org/10.3389/fenrg.2022.871617

Jing, H. H., Bardakci, F., Akgöl, S., Kusat, K., Adnan, M., Alam, M. J., Gupta, R., Sahreen, S., Chen, Y., Gopinath, S. C. B., & Sasidharan, S. (2023). *Green Carbon Dots: Synthesis, Characterization, Properties and Biomedical Applications*. https://doi.org/10.3390/jfb14010027

Kansay, V., Sharma, V. D., Chandan, G., Sharma, I., Bhatia, A., Chakrabarti, S., & Bera, M. K. (2023). Sustainable synthesis and characterization of fluorescent nanoprobe based on unintentional heteroatom doped-carbon quantum dots for bioimaging of human neuroblastoma cancer cells and living organisms. *Journal of Photochemistry and Photobiology A: Chemistry*, *443*(January), 114879. https://doi.org/10.1016/j.jphotochem.2023.114879

Karuppasamy, B. D., Perumal, S., Atchudan, R., Sundramoorthy, A. K., Manoj, D., Sambasivam, S., Karthik, N., Kamaraj, E., Suresh Kumar, R., Ramalingam, S., & Rok Lee, Y. (2024). Eco-friendly Coccinia Grandis-derived excitation-dependent fluorescence of carbon dots for In-Vivo bioimaging and fluorescent ink applications. *Materials Science and Engineering: B*, *303*, 117300. https://doi.org/10.1016/J.MSEB.2024.117300

Karuppasamy, B. D., Perumal, S., Atchudan, R., Sundramoorthy, A. K., Ramalingam, S., Manoj, D., Sangaraju, S., Jebakumar Immanuel Edison, T. N., Lee, S. W., & Lee, Y. R. (2025a). Hydrothermal synthesis of intrinsic carbon dots with tunable emission for fluorescent inks and variegated bioimaging applications. *Journal of Molecular Liquids*, *437*, 128592. https://doi.org/10.1016/J.MOLLIQ.2025.128592

Karuppasamy, B. D., Perumal, S., Atchudan, R., Sundramoorthy, A. K., Ramalingam, S., Manoj, D., Sangaraju, S., Jebakumar Immanuel Edison, T. N., Lee, S. W., & Lee, Y. R. (2025b). Hydrothermal synthesis of intrinsic carbon dots with tunable emission for fluorescent inks and variegated bioimaging applications. *Journal of Molecular Liquids*, *437*(PC), 128592. https://doi.org/10.1016/j.molliq.2025.128592

Kasirajan, K., Karunakaran, M., & Choi, H. K. (2024). Synthesis of environmentally-friendly carbon quantum dots from orange juice for selective detection of Fe3+ ions,

antibacterial activity, and bio-imaging applications. *Journal of Environmental Chemical Engineering*, *12*(5), 113535. https://doi.org/10.1016/j.jece.2024.113535

Kausar, A. (2019). Polymer/carbon-based quantum dot nanocomposite: forthcoming materials for technical application. *Journal of Macromolecular Science, Part A*, *56*(4), 341–356. https://doi.org/10.1080/10601325.2019.1578614

Krishnaiah, P., Atchudan, R., Gangadaran, P., Perumal, S., Rajendran, R. L., Sundramoorthy, A. K., Suresh Kumar, R., Ramalingam, S., Ahn, B. C., Lee, S. W., & Lee, Y. R. (2025). A sustainable synthesis and applications of biomass waste-derived tunable fluorescent carbon dots: In vitro and in vivo fluorescent imaging. *Journal of Photochemistry and Photobiology A: Chemistry*, *458*, 115944. https://doi.org/10.1016/J.JPHOTOCHEM.2024.115944

Kumar, M., Chinnathambi, S., Bakhori, N., Abu, N., Etezadi, F., Thangavel, V., Packwood, D., Sivaniah, E., & Pandian, G. N. (2024). Biomass-derived carbon dots as fluorescent quantum probes to visualize and modulate inflammation. *Scientific Reports*, *14*(1), 12665. https://doi.org/10.1038/s41598-024-62901-7

Leary, J., & Key, J. (2014). Nanoparticles for multimodal in vivo imaging in nanomedicine. *International Journal of Nanomedicine*, 711. https://doi.org/10.2147/IJN.S53717

Lee, S. J., Zheng, Y. Y., Chen, W. M., & Hsueh, Y. H. (2024). Nitrogen-Doped Carbon Dots: A New Powerful Fluorescent Dye with Substantial Effect on Bacterial Cell Labeling. *ACS Omega*. https://doi.org/10.1021/acsomega.4c04273

Liu, J., Li, R., & Yang, B. (2020). Carbon Dots: A New Type of Carbon-Based Nanomaterial with Wide Applications. *ACS Central Science*, *6*(12), 2179–2195. https://doi.org/10.1021/acscentsci.0c01306

Liu, Y., Su, X., Chen, L., Liu, H., Zhang, C., Liu, J., Hao, J., Shangguan, Y., & Zhu, G. (2021). Green preparation of carbon dots from Momordica charantia L. for rapid and effective sensing of p-aminoazobenzene in environmental samples. *Environmental Research*, *198*, 111279. https://doi.org/10.1016/J.ENVRES.2021.111279

Liu, G., Wang, H., Dong, J., He, Y., Wang, R., Li, X., Liu, D., Duan, J., Feng, J., Lu, X., Gui, L., Hou, S., Liu, Z., Peng, H., & Zhu, Y. (2025a). High-yield synthesis of biomass-derived carbon dots for enhanced taraxacum growth. *Biomass and Bioenergy*, *203*, 108351. https://doi.org/10.1016/J.BIOMBIOE.2025.108351

Liu, Q., Chen, H., Mi, R., Min, X., Fang, M., Wu, X., Huang, Z., & Liu, Y. (2025b). Biomass-Derived Carbon Dots: Preparation, Properties, and Applications. *Nanomaterials*, *15*(16), 1279. https://doi.org/10.3390/nano15161279

Liu, Z. F., Wang, J. H., Wang, C. P., Wang, Q., Li, J., Han, C. J., & Lu, Z. Y. (2025c). Green hydrothermal valorization of Rosa damascena Mill. floral waste into functional carbon dots for anti-inflammatory nanomedicine. *Industrial Crops and Products*, *236*, 122115. https://doi.org/10.1016/J.INDCROP.2025.122115

Louw, C. J., de Haan, P., Verpoorte, E., & Baker, P. (2025). Carbon quantum dots as a co-reactant to Ru(bpy)32+ for electrochemiluminescence biosensing of cardiac troponin I. *Electrochimica Acta*, *542*, 147516. https://doi.org/10.1016/J.ELECTACTA.2025.147516

Luo, W.-K., Zhang, L.-L., Yang, Z.-Y., Guo, X.-H., Wu, Y., Zhang, W., Luo, J.-K., Tang, T., & Wang, Y. (2021). Herbal medicine derived carbon dots: synthesis and applications in therapeutics, bioimaging and sensing. *Journal of Nanobiotechnology*, *19*(1), 320. https://doi.org/10.1186/s12951-021-01072-3

Mahto, V. K., Singh, V. K., Singh, V. K., Singh, A., Singh, S., Mehara, A. K., Rajak, N., Mishra, A., Garg, N., Upadhyay, A., Rai, A., & Singh, A. K. (2025). Green single-step hydrothermal synthesis of fluorescent carbon dots from Lantana camara flower for the effective fluorescent detection of Cr(VI) and live cell imaging. *Biomass Conversion and Biorefinery*, *15*(11), 16857–16870. https://doi.org/10.1007/s13399-024-06384-6

Mailisa, W., Annisa, W. D., Permatasari, F. A., Amalia, R., Ivansyah, A. L., Iskandar, F., & Rachmawati, H. (2023). In Vitro and Silico Studies on the N-Doped Carbon Dots Potential in ACE2 Expression Modulation. *ACS Omega*, *8*(11), 10077–10085. https://doi.org/10.1021/acsomega.2c07398

Malik, S., Muhammad, K., & Waheed, Y. (2023). Emerging Applications of Nanotechnology in Healthcare and Medicine. *Molecules*, *28*(18), 6624. https://doi.org/10.3390/molecules28186624

Mancini, F., Menichetti, A., Degli Esposti, L., Montesi, M., Panseri, S., Bassi, G., Montalti, M., Lazzarini, L., Adamiano, A., & Iafisco, M. (2023). Fluorescent Carbon Dots from Food Industry By-Products for Cell Imaging. *Journal of Functional Biomaterials*, *14*(2). https://doi.org/10.3390/jfb14020090

Manjubaashini, N., Bargavi, P., & Balakumar, S. (2024a). Carbon quantum dots derived from agro waste biomass for pioneering bioanalysis and in vivo bioimaging. *Journal of Photochemistry and Photobiology A: Chemistry*, *454*(April), 115702. https://doi.org/10.1016/j.jphotochem.2024.115702

Manjubaashini, N., Bargavi, P., & Balakumar, S. (2024b). Carbon quantum dots derived from agro waste biomass for pioneering bioanalysis and in vivo bioimaging. *Journal of Photochemistry and Photobiology A: Chemistry*, *454*, 115702. https://doi.org/10.1016/J.JPHOTOCHEM.2024.115702

Mansuriya, B. D., & Altintas, Z. (2021). Carbon dots: Classification, properties, synthesis, characterization, and applications in health care-an updated review (2018–2021). *Nanomaterials*, *11*(10). https://doi.org/10.3390/nano11102525

Mohammed, S. J., Sidiq, M. K., Najmuldeen, H. H., Kayani, K. F., Kader, D. A., & Aziz, S. B. (2024). A comprehensive review on nitrogen-doped carbon dots for antibacterial applications. *Journal of Environmental Chemical Engineering*, *12*(6), 114444. https://doi.org/10.1016/j.jece.2024.114444

Molaei, M. J. (2019). Carbon quantum dots and their biomedical and therapeutic applications: a review. *RSC Advances*, *9*(12), 6460–6481. https://doi.org/10.1039/C8RA08088G

Mou, Z., Yang, Q., Zhao, B., Li, X., Xu, Y., Gao, T., Zheng, H., Zhou, K., & Xiao, D. (2021). Scalable and Sustainable Synthesis of Carbon Dots from Biomass as Efficient Friction Modifiers for Polyethylene Glycol Synthetic Oil. *ACS Sustainable Chemistry & Engineering*, *9*(44), 14997–15007. https://doi.org/10.1021/acssuschemeng.1c05678

Murugan, R., Tamil Selvan, S., Subramanian, R., S, C., & Ali, S. (2024). Sustainable carbon quantum dots enhanced photoluminescence for bioimaging applications: An in vitro and in silico analysis. *Journal of Photochemistry and Photobiology A: Chemistry*, *453*, 115669. https://doi.org/10.1016/J.JPHOTOCHEM.2024.115669

Napporn, T. W., Canaff, C., Bere, E., & Hacker, V. (2018). Characterization Methods for Components and Materials. In *Fuel Cells and Hydrogen* (pp. 155–173). Elsevier. https://doi.org/10.1016/B978-0-12-811459-9.00008-6

Naziba, T. A., Kumar, D. P., Karthikeyan, S., Sriramajayam, S., Djanaguiraman, M., Sundaram, S., Ghamari, M., Rao, R. P., Ramakrishna, S., & Ramesh, D. (2024). Biomass Derived Biofluorescent Carbon Dots for Energy Applications: Current Progress and Prospects. *The Chemical Record*, *24*(6). https://doi.org/10.1002/tcr.202400030

Ngara, Z. S., Refli, Pingak, R. K., Bukit, M., Bernandus, Tarigan, J., & Lerrick, R. I. (2025). Characterization and application of fluorescent carbon NANODOTS from dragon fruit peel as probes for detection of metal ions. *Results in Chemistry*, *17*, 102522. https://doi.org/10.1016/J.RECHEM.2025.102522

Ou, S. F., Zheng, Y. Y., Lee, S. J., Chen, S. T., Wu, C. H., Hsieh, C. Te, Juang, R. S., Peng, P. Z., & Hsueh, Y. H. (2021). N-doped carbon quantum dots as fluorescent bioimaging agents. *Crystals*, *11*(7). https://doi.org/10.3390/cryst11070789

Owsianiak, M., Ryberg, M. W., Renz, M., Hitzl, M., & Hauschild, M. Z. (2016). Environmental Performance of Hydrothermal Carbonization of Four Wet Biomass Waste Streams at Industry-Relevant Scales. *ACS Sustainable Chemistry & Engineering*, *4*(12), 6783–6791. https://doi.org/10.1021/acssuschemeng.6b01732

Pal, D., Das, P., Ghosh, P., Mondal, S., Halder, S., Basak, P., & Nandi, S. K. (2025). Waste-derived marigold flower carbon dot spray and gel formulations exhibit enhanced wound healing in deep excisional cutaneous and burn wounds. *Journal of Materials Chemistry B*, *13*(20), 5919–5932. https://doi.org/10.1039/D5TB00323G

Papan Djaniš, J., Szymczak, M., Hočevar, J., Iskra, J., Genorio, B., Lisjak, D., Marciniak, L., & Elzbieciak-Piecka, K. (2026). Exploring the interplay between formation mechanisms and luminescence of lignin carbon quantum dots from spruce biomass. *Dyes and Pigments*, *246*, 113301. https://doi.org/10.1016/J.DYEPIG.2025.113301

Parray, A. H., Sohal, N., Singh, P., & Kolte, J. (2026). Green synthesis of carbon quantum dots from biomass: A sustainable approach to nanotechnology. *Biomass and Bioenergy*, *204*, 108447. https://doi.org/10.1016/J.BIOMBIOE.2025.108447

Patel, P. J., Gupte, S., Naik, R., Kailasa, S. K., Jha, S., Patel, S. B., & Mehta, V. N. (2024). Fruit Peel Derived Carbon Dots for Improved Curcumin Delivery: A Promising Strategy for Enhanced Antimicrobial and Antioxidant Activity. *ChemistrySelect*, *9*(32). https://doi.org/10.1002/slct.202400762

Pathak, R., Punetha, V. D., Bhatt, S., & Punetha, M. (2023). Multifunctional role of carbon dot-based polymer nanocomposites in biomedical applications: a review. *Journal of Materials Science*, *58*(15), 6419–6443. https://doi.org/10.1007/s10853-023-08408-4

Qin, J., Gao, X., Chen, Q., Liu, H., Liu, S., Hou, J., & Sun, T. (2021). PH sensing and bioimaging using green synthesized carbon dots from black fungus. *RSC Advances*, *11*(50), 31791–31794. https://doi.org/10.1039/d1ra05199g

Ren, J., Weber, F., Weigert, F., Wang, Y., Choudhury, S., Xiao, J., Lauermann, I., Resch-Genger, U., Bande, A., & Petit, T. (2019). Influence of surface chemistry on optical, chemical and electronic properties of blue luminescent carbon dots. *Nanoscale*, *11*(4), 2056–2064. https://doi.org/10.1039/C8NR08595A

Ren, X., Zhang, F., Guo, B., Gao, N., & Zhang, X. (2019). Synthesis of N-doped Micropore carbon quantum dots with high quantum yield and dual-wavelength photoluminescence emission from biomass for cellular imaging. *Nanomaterials*, *9*(4), 22–25. https://doi.org/10.3390/nano9040495

Ribet, S. M., Murthy, A. A., Roth, E. W., dos Reis, R., & Dravid, V. P. (2021). Making the most of your electrons: Challenges and opportunities in characterizing hybrid interfaces with STEM. *Materials Today*, *50*, 100–115. https://doi.org/10.1016/j.mattod.2021.05.006

Salvi, A., Kharbanda, S., Thakur, P., Shandilya, M., & Thakur, A. (2024). Biomedical application of carbon quantum dots: A review. *Carbon Trends*, *17*, 100407. https://doi.org/10.1016/J.CARTRE.2024.100407

Sambudi, N. S., Mulia, M. G., Khayrani, A. C., Isnaeni, Raviadaran, R., Aziz, F., Permana, D. D., Suwandi, R., & Lischer, K. (2025). Production of Carbon Quantum Dots Based on Oil Palm Fronds for Polyethylene and Polyethylene Terephthalate Microplastics Detection. *International Journal of Technology*, *16*(1), 233–242. https://doi.org/10.14716/ijtech.v16i1.7376

Shahraki, H. S., Bushra, R., Shakeel, N., Ahmad, A., Quratulen, Ahmad, M., & Ritzoulis, C. (2023). Papaya peel waste carbon dots/reduced graphene oxide nanocomposite: From photocatalytic decomposition of methylene blue to antimicrobial activity. *Journal of Bioresources and Bioproducts*, *8*(2), 162–175. https://doi.org/10.1016/J.JOBAB.2023.01.009

Shen, F., Lu, Z., Yan, K., Luo, K., Pei, S., & Xiang, P. (2025). Synthesis and properties of carbon quantum dots as an antimicrobial agent and detection of ciprofloxacin. *Scientific Reports*, *15*(1), 1–10. https://doi.org/10.1038/s41598-025-14383-4

Shi, C., Qi, H., Ma, R., Sun, Z., Xiao, L., Wei, G., Huang, Z., Liu, S., Li, J., Dong, M., Fan, J., & Guo, Z. (2019). N,S-self-doped carbon quantum dots from fungus fibers for sensing tetracyclines and for bioimaging cancer cells. *Materials Science and Engineering C*, *105*(August), 110132. https://doi.org/10.1016/j.msec.2019.110132

Shi, W., Li, J., Pu, J., Cheng, G., Liu, Y., Xiao, S., & Cao, J. (2025). Epigynum auritum-Derived Near-Infrared Carbon Dots for Bioimaging and Antimicrobial Applications. *Molecules*, *30*(2). https://doi.org/10.3390/molecules30020422

Shukla, D., Das, M., Kasade, D., Pandey, M., Dubey, A. K., Yadav, S. K., & Parmar, A. S. (2020). Sandalwood-derived carbon quantum dots as bioimaging tools to investigate the

toxicological effects of malachite green in model organisms. *Chemosphere*, *248*, 125998. https://doi.org/10.1016/j.chemosphere.2020.125998

Solis Flores, S., López-Pacheco, I. Y., Villalba-Rodriguez, A. M., González-González, R. B., Parra-Saldívar, R., & Iqbal, H. M. N. (2024). Effect of carbon dots supplementation in Chlorella vulgaris biomass production and its composition. *Nano Express*, *5*(2), 025007. https://doi.org/10.1088/2632-959X/ad3cfd

Stachurski, C. D., Click, S. M., Wolfe, K. D., Dervishogullari, D., Rosenthal, S. J., Jennings, G. K., & Cliffel, D. E. (2020). Optical and electrochemical tuning of hydrothermally synthesized nitrogen-doped carbon dots. *Nanoscale Advances*, *2*(8), 3375–3383. https://doi.org/10.1039/d0na00264j

Stevie, F. A., & Donley, C. L. (2020). Introduction to x-ray photoelectron spectroscopy. *Journal of Vacuum Science & Technology A: Vacuum, Surfaces, and Films*, *38*(6). https://doi.org/10.1116/6.0000412

Sturabotti, E., Sierra-Serrano, B., Apresto, S. M., Cesco, M., Comparini, L., Cardo, L., & Prato, M. (2025). Carbon dots as multi-modal contrast agents: opportunities and open challenges for in vivo bioimaging. *Advanced Drug Delivery Reviews*, *224*, 115659. https://doi.org/10.1016/J.ADDR.2025.115659

Sun, H., Zhang, W., Xie, J., Sun, M., Hu, P., Zhang, Z., Zhu, J., Zhao, Y., & Liu, L. (2025). IFE and Dynamic Quenching mediated fluorescent sensing of Cr(Ⅵ) based on nitrogen-doped biomass carbon dots. *Environmental Research*, *286*, 123024. https://doi.org/10.1016/J.ENVRES.2025.123024

Sun, X., & Li, Y. (2004). Colloidal Carbon Spheres and Their Core/Shell Structures with Noble-Metal Nanoparticles. *Angewandte Chemie International Edition*, *43*(5), 597–601. https://doi.org/10.1002/anie.200352386

United States Environmental Protection Agency. (2024). *Percentage of biomass waste in developed countries*. https://www.epa.gov/facts-and-figures-about-materials-waste-and-recycling

Vinayagam, R., Shetty, S. A., Murugesan, G., Goveas, L. C., Varadavenkatesan, T., & Selvaraj, R. (2025). Peltophorum pterocarpum flower mediated synthesis of silver nanoparticles and its catalytic degradation of Acid Blue 113 dye. *Scientific Reports*, *15*(1), 26452. https://doi.org/10.1038/s41598-025-11980-1

Wang, B., Cai, H., Waterhouse, G. I. N., Qu, X., Yang, B., & Lu, S. (2022). Carbon Dots in Bioimaging, Biosensing and Therapeutics: A Comprehensive Review. *Small Science*, *2*(6). https://doi.org/10.1002/smsc.202200012

Wang, D., Dong, H., Ren, L., Jiang, Y., Xi, L., Li, X., Cui, F., Li, T., & Li, J. (2025). Carbon dots in health protection: mechanisms and applications. *Food Chemistry*, *492*, 145544. https://doi.org/10.1016/J.FOODCHEM.2025.145544

Wang, Q., Li, H., Chen, L., & Huang, X. (2001). Monodispersed hard carbon spherules with uniform nanopores. *Carbon*, *39*(14), 2211–2214. https://doi.org/10.1016/S0008-6223(01)00040-9

Wang, Z., Chen, D., Gu, B., Gao, B., Wang, T., Guo, Q., & Wang, G. (2020). Biomass-derived nitrogen doped graphene quantum dots with color-tunable emission for sensing, fluorescence ink and multicolor cell imaging. *Spectrochimica Acta - Part A: Molecular and Biomolecular Spectroscopy*, *227*, 117671. https://doi.org/10.1016/j.saa.2019.117671

Wechakorn, K., Khaopueak, P., Seesuea, C., Leung, F. K. C., & Tantipanjaporn, A. (2025). Facile green synthesis of multifunctional carbon dots from cassava peel for heavy metal ion sensing, photocatalytic degradation, antioxidant activity, and fluorescence bioimaging. *Materials Science and Engineering: B*, *320*, 118435. https://doi.org/10.1016/J.MSEB.2025.118435

Wijayanti, N. PAD., Permatasari, F. A., Damayanti, S., Anggadiredja, K., Iskandar, F., Wibowo, I., & Rachmawati, H. (2024). Toxicity assessment and bioimaging potential of carbon dots synthesized from banana peel in zebrafish model. *Narra J*, *4*(3), e1228. https://doi.org/10.52225/narra.v4i3.1228

Xiang, J., Chen, X., Liu, Q., Jing, H., Chen, T., Tang, W., & Xu, W. (2023). Synthesis of Carbon dots from Biomass Chenpi for the Detection of Hg2+. *Journal of Renewable Materials*, *11*(10), 3739–3750. https://doi.org/10.32604/jrm.2023.028090

Yang, C., Ren, W., Qian, J., Chen, F., & Cao, F. (2025). Study on the properties of biomass carbon quantum dots modified with diamine compounds and their application in iron ion detection. *Fullerenes, Nanotubes and Carbon Nanostructures*, *33*(7), 740–753. https://doi.org/10.1080/1536383X.2025.2450299

Yao, Y., Zhang, T., & Tang, M. (2023). The DNA damage potential of quantum dots: Toxicity, mechanism and challenge. *Environmental Pollution*, *317*, 120676. https://doi.org/10.1016/j.envpol.2022.120676

Yoda, K., Koide, R., Koizumi, K., Oikawa, M., Miyazaki, Y., Sun, L., Yoshizawa, N., & Wang, Z.-M. (2026). New insights into the mechanisms of biomass-derived carbon quantum dots for photocatalytic disinfection. *Carbon*, *246*, 120836. https://doi.org/10.1016/J.CARBON.2025.120836

Yuan, L., Shao, C., Zhang, Q., Webb, E., Zhao, X., & Lu, S. (2024). Biomass-derived carbon dots as emerging visual platforms for fluorescent sensing. *Environmental Research*, *251*, 118610. https://doi.org/10.1016/J.ENVRES.2024.118610

Zhang, Q., Tian, F., Zhou, Q., Zhang, C., Tang, S., Jiang, L., & Du, S. (2022). Targeted ginkgo kernel biomass precursor using eco-friendly synthesis of efficient carbon quantum dots for detection of trace nitrite ions and cell imaging. *Inorganic Chemistry Communications*, *140*(December 2021), 109442. https://doi.org/10.1016/j.inoche.2022.109442

Zhang, Y., Li, Z., Sheng, L., & Meng, A. (2023). Lemon juice-derived nitrogen-doped carbon quantum dots for highly sensitive and selective determination of ferrous ions and cell imaging. *Colloids and Surfaces A: Physicochemical and Engineering Aspects*, *657*(PA), 130580. https://doi.org/10.1016/j.colsurfa.2022.130580

Zhao, S.-S., Wang, Y., Yang, Z., Liu, X., Yang, Z., Jia, X., Song, C., Wang, Y.-B., & Chen, X. (2021). Hydrothermal Synthesis of Carbon Dots from Luochuan Red Fuji Apple Peel and Application for the Detection of Fe3+ Ions. *Nano*, *16*(13). https://doi.org/10.1142/S1793292021501563

Zheng, K., Li, X., Chen, M., Gong, Y., Tang, A., Wang, Z., Wei, Z., Guan, L., & Teng, F. (2020). Controllable synthesis highly efficient red, yellow and blue carbon nanodots for photo-luminescent light-emitting devices. *Chemical Engineering Journal*, *380*, 122503. https://doi.org/10.1016/J.CEJ.2019.122503

Zhou, J., Ge, M., Han, Y., Ni, J., Huang, X., Han, S., Peng, Z., Li, Y., & Li, S. (2020). Preparation of Biomass-Based Carbon Dots with Aggregation Luminescence Enhancement from Hydrogenated Rosin for Biological Imaging and Detection of $Fe^{3+}$. *ACS Omega*, *5*(20), 11842–11848. https://doi.org/10.1021/acsomega.0c01527

Zhou, Y., Mintz, K. J., Sharma, S. K., & Leblanc, R. M. (2019). Carbon Dots: Diverse Preparation, Application, and Perspective in Surface Chemistry. *Langmuir*, *35*(28), 9115–9132. https://doi.org/10.1021/acs.langmuir.9b00595

## Biographies of Author

**Yuni Aldriani Lubis,** a freshgraduate of master of chemistry, a lecturer and reseach assistant of physical chemistry laboratory at Universitas Sumatera Utara. I understand the fields of physical chemistry, materials, quantum dots, sensors, natural rubber latex, and other nanomaterial fields.

- Email: yunialdrianil@gmail.com
- ORCID: 0009-0009-1494-6861
- Web of Science ResearcherID: N/A
- Scopus Author ID: N/A
- Homepage: N/A